Active motions of Brownian particles in a generalized energy-depot model

2008 New J. Phys. 10 103018

(http://iopscience.iop.org/1367-2630/10/10/103018)

New Journal of Physics
The open-access journal for physics

Active motions of Brownian particles in a generalized energy-depot model

Yong Zhang[1], **Chul Koo Kim**[1,4] **and Kong-Ju-Bock Lee**[2,3,4]
[1] Institute of Physics and Applied Physics, Yonsei University, Seoul 120-749, Korea
[2] Department of Physics, Ewha Woman's University, Seoul 120-750, Korea
[3] School of Physics, Korea Institute for Advanced Study, Seoul 130-722, Korea
E-mail: xyzhang@phya.yonsei.ac.kr, ckkim@yonsei.ac.kr and kjblee@ewha.ac.kr

New Journal of Physics **10** (2008) 103018 (17pp)
Received 9 June 2008
Published 16 October 2008
Online at http://www.njp.org/
doi:10.1088/1367-2630/10/10/103018

Abstract. We present a generalized energy-depot model in which the rate of conversion of the internal energy into motion can be dependent on the position and velocity of a particle. When the conversion rate is a general function of the velocity, the active particle exhibits diverse patterns of motion, including a braking mechanism and a stepping motion. The phase trajectories of the motion are investigated in a systematic way. With a particular form of the conversion rate dependent on the position and velocity, the particle shows a spontaneous oscillation characterizing a negative stiffness. These types of active behaviors are compared with similar phenomena observed in biology, such as the stepping motion of molecular motors and amplification in the hearing mechanism. Hence, our model can provide a generic understanding of the active motion related to the energy conversion and also a new control mechanism for nano-robots. We also investigate the effect of noise, especially on the stepping motion, and observe random walk-like behavior as expected.

[4] Authors to whom any correspondence should be addressed.

Contents

1. Introduction

Active motion is a phenomenon found ubiquitously in nature, ranging from the colony organization of microorganisms, biological springs, molecular motors, nano-robotics [1]–[5] and flocking of fish and birds to the swarming of small insects [6, 7]. All these types of active motions need processes of energy supply, conversion to motion, and resupply for repeated motions. To describe these processes, an energy-depot model was introduced by Schweitzer *et al* [8, 9]. In the energy-depot model, the supplied energy is able to induce effectively a negative friction in a certain range of velocity, yielding an active motion. This model was successfully applied to a wide variety of active motions [3, 4], [8]–[12] mainly assuming that the rate of energy conversion into motion depends only on the quadratic form of the velocity. The success of the quadratic energy conversion rate model immediately raises the possibility that other diverse active motions could be induced when the energy conversion rate contains various terms in velocity, including the quadratic one.

Another motivation for the present study originates from the fields of nano-robotics and artificial molecular motions [5, 13]. Rapid developments in these areas require diverse controlling technology for energy conversion for the intended purpose. Although at present it is still at a primitive stage, control of the energy conversion will become fine-tuned in the near future so that any desired motion could be selectively achieved. Motivated by these considerations, we consider various forms of the rate of conversion of the internal energy into motion in this paper. Hence our work provides a correlation between the form of energy conversion and the active motion.

In the following sections, we introduce our generalized energy-depot model in detail and consider various forms of the conversion rate that could induce diverse active motions including a braking mechanism applicable to nonlinear compressive behavior of the basilar membrane (BM) in the inner ear [14], a directed stepping motion shown by molecular motor systems [15]–[17], or the phenomenon of negative stiffness for oscillatory systems such as hair bundles in mammals [18]. Concluding remarks will follow.

2. The generalized energy-depot model

A Brownian particle moving in an external force $f(x)$ is governed by the Langevin equation,

$$m\frac{\mathrm{d}v}{\mathrm{d}t} = -\mu_0 v + f(x) + \sqrt{2k_\mathrm{B}T\mu_0}\zeta(t), \tag{1}$$

where m is the mass, v is the velocity of the particle, μ_0 is the friction coefficient, T is the temperature, and the white noise, $\zeta(t)$, satisfies $\langle\zeta(t)\rangle = 0$ and $\langle\zeta_i(t)\zeta_j(t')\rangle = \delta_{ij}\delta(t-t')$. The passive motion can be converted to active motion when the internal energy depot is introduced. The internal energy of the depot, $e(t)$, is regarded as an additional degree of freedom for each particle. The energy balance equation for the depot can be described as [9]

$$\alpha\frac{\mathrm{d}e(t)}{\mathrm{d}t} = q(x) - ce(t) - d(x,v)e(t), \tag{2}$$

where α is the timescale of relaxation of the depot, q the rate of the energy influx to the depot, c the rate of energy dissipation of the depot, and $d(x,v)$ the conversion rate of the internal energy into motion. $\alpha = 1$ means that the depot reacts with a time lag and $\alpha \to 0$ means that the depot adapts very fast (adiabatic approximation). We note that the rate of conversion of the internal energy into motion can be, in general, a function of both the velocity and position of the particle, which contains various combinations of the two variables [8, 9, 19, 20]. In order to understand the roles of the individual terms, we expand $d(x,v)$ as follows:

$$d(x,v) = \sum_{i,j=0}^{\infty} a_{i,j}x^i v^j. \tag{3}$$

We can choose $a_{0,0} = 0$ since the effect of constant conversion rate can be merged into the constant dissipation rate.

Consequently, the Langevin equation for an active Brownian particle is written as

$$\begin{aligned} m\frac{\mathrm{d}v}{\mathrm{d}t} &= -\mu_0 v + f(x) + F_\mathrm{active} + \sqrt{2k_\mathrm{B}T\mu_0}\zeta(t), \\ &= -\mu(x,v)v + f(x) + \sqrt{2k_\mathrm{B}T\mu}\zeta(t), \end{aligned} \tag{4}$$

where $F_\mathrm{active} = d(x,v)e(t)/v$ and $\mu(x,v) = \mu_0 - d(x,v)e(t)/v^2$. The above equations are intuitive in the sense that the Brownian particle is governed by an extra active force or that the friction is modified to depend on the space and velocity, when external energy is supplied. It is noticeable that the effective friction can be negative or larger than the normal friction μ_0. The effective friction will be discussed in detail in the next section.

In this paper, q and c are assumed to be constant for the sake of simplicity, and the main focus is on the effect of the conversion rate. For this purpose, we consider the conversion rate $d(v)$ depending only on the velocity first and we consider $d(x,v)$ in a special form later. Even when only velocity-dependent conversion rate is considered, diverse properties can be discussed such as the motion with a braking mechanism, the stability of fixed points, and a stepping motion. A special form of $d(x,v)$ is chosen to describe the possibility of a negative stiffness.

3. Motion with a braking mechanism

The active Brownian particle with $d(v) \sim v^2$ has previously been treated in detail and it was shown that the friction can be effectively negative when the particle moves slowly and increases

only up to μ_0 as the particle moves faster [8, 9]. Hence, for an active particle with $d(v) \sim v^2$, the speed can be increased without any limit. Since such an excessive speed can damage living organisms, it may be possible that a living organism is equipped with a protective mechanism to prevent damage from excessive movement or energy pumping, especially in underdamped oscillating systems. Also, in nano-robotics, adoption of this type of protective mechanism may be not only helpful to control the movement, but also essential to safeguard the mechanism from overdriving. Thus, studies on the contributions of higher order velocity terms are highly desirable.

Motivated by these arguments, we first study a symmetric form including up to the fourth order term in the rate of conversion of the internal energy into motion. Hence,

$$d(v) = a_{0,2}v^2 + a_{0,4}v^4, \tag{5}$$

where the positive (negative) $a_{0,4}$ increases (decreases) the kinetic energy of the particle. Since we are interested in the braking mechanism, only the negative case will be treated. By introducing a critical velocity, $v_c = \sqrt{a_{0,2}/|a_{0,4}|}$, the conversion rate is rewritten as

$$d(v) = a_{0,2}v^2\left(1 - \frac{v^2}{v_c^2}\right). \tag{6}$$

This implies that the energy depot reabsorbs the kinetic energy when the velocity goes beyond the critical velocity. This mechanism is analogous to the regenerative-brake system in automobiles and electric vehicles [21]. It is shown that this regenerative-braking can not only control the motion more effectively, but also save energy for operation. Thus, we name this fourth order model a Brownian energy-depot model with a braking mechanism.

To describe the effect of the fourth order term on the conversion rate, let us consider an adiabatic approximation, $\alpha \to 0$, in which the energy depot adapts very fast. The adiabatic solution of the internal energy of depot yields [9]

$$e(t) = \frac{q}{c + a_{0,2}\left(1 - v^2/v_c^2\right)v^2}. \tag{7}$$

Hence the effective friction coefficient becomes

$$\begin{aligned}\mu(v) &= \mu_0 - \frac{d(v)}{v^2}e(t) \\ &= \mu_0 - \frac{q a_{0,2}(1 - v^2/v_c^2)}{c + a_{0,2}(1 - v^2/v_c^2)v^2}.\end{aligned} \tag{8}$$

Note that $\mu(v_c) = \mu_0$. The effective friction describes three different situations: (i) pumping, where $\mu(v) < 0$, (ii) dissipation, where $0 < \mu(v) < \mu_0$, and (iii) protection, where $\mu_0 < \mu(v)$ (figure 1). The particle cannot speed up when the velocity exceeds the critical velocity in this model, since the fourth order term in the conversion rate induces sufficiently large friction to the particle. Superficially, the present model appears to be similar to the Rayleigh model [22], but with different interpretations.

We believe that the newly introduced braking mechanism may offer a plausible way to discuss any underdamped motions and protection from any overreacting motion in living organisms and nano-robotics. Recently, by adopting this mechanism to the active oscillation of the BM in the mammalian ear, we could successfully explain the known experimental results and the noise amplification in cochlea [14].

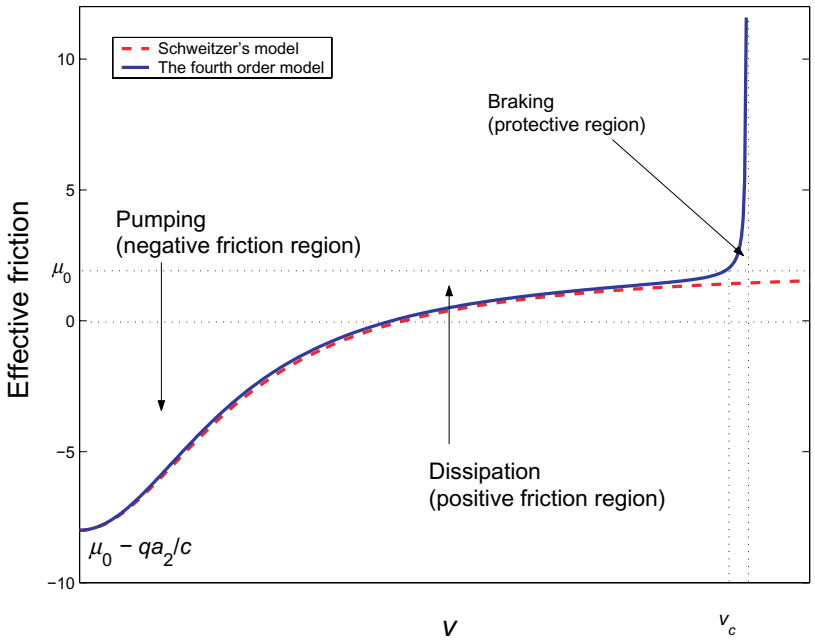

Figure 1. An illustration of the effective friction as a function of the velocity. The solid line shows the effect of the fourth order term on the conversion rate, compared with the Schweitzer's result in the dashed line. $q = 10$, $\mu_0 = 2.0$, $v_c = 5.0$ and $a_{0,2}/c = 1$ are used for the numerical calculation.

4. Stability of fixed points

So far, we have restricted the conversion rate $d(v)$ to be symmetric in velocity. However, the active particles generally possess polarities in their motions [5, 13], [15]–[17]. The polarity of the motion has originated from the external force and/or the asymmetric conversion rate. To discuss the generic polarity of the motion, in this section, we consider a general form of $d(v)$,

$$d(v) = a_{0,1}v + a_{0,2}v^2 + a_{0,3}v^3 + a_{0,4}v^4 + \cdots. \tag{9}$$

It is expected that inclusion of these odd terms allows the active particles to perform polarized motions as observed in molecular motors such as kinesin and dynein. Now, it is worth analyzing the deterministic dynamics in the $\{v, e\}$ phase space, which is governed by

$$\begin{aligned} \dot{v} &= -\frac{\mu_0}{m}v + \frac{f}{m} + \frac{d(v)}{mv}e, \\ \dot{e} &= q - ce - d(v)e, \end{aligned} \tag{10}$$

where the depot takes time to be filled with energy ($\alpha = 1$). It is well known that the long-time behavior of a two-dimensional continuous dynamical system possesses only fixed points and limit cycles [23]. Although it is not possible to describe the solution analytically, local stability for existing fixed points can be analyzed through the Jacobian matrix and its eigenvalues [9, 23]. In the following, we discuss the stability of the fixed points obtained numerically for various values of $a_{i,j}$. For the numerical calculation, $m = 1$, $q = 10$, $c = 0.01$ and $\mu_0 = 20$ are used.

Table 1 shows the bifurcation with the variation of $a_{0,3}$ when we consider the conversion rate only up to the third order of velocity and there is no external force. There is always at least

Table 1. Bifurcation with a variation of $a_{0,3}$, when $d(v) = a_{0,1}v + a_{0,2}v^2 + a_{0,3}v^3$, $a_{0,1} = 0.0002$, $a_{0,2} = 2.0$ and $f = 0$. Here, $(+/-)$ denotes positive/negative velocity.

Range of $a_{0,3}$	Classification of the fixed point(s)
$a_{0,3} \leqslant -0.93$	• One unstable focal fixed point $(-)$ • One saddle point $(-)$ • One stable fixed point $(+)$
$-0.93 < a_{0,3} < -0.16$	• One unstable focal fixed point $(-)$ • One saddle point $(-)$ • One stable focal fixed point $(+)$
$-0.16 \leqslant a_{0,3} < 0.16$	• One stable focal fixed point $(-)$ • One saddle point $(-)$ • One stable focal fixed point $(+)$
$0.16 \leqslant a_{0,3} < 0.93$	• One stable focal fixed point $(-)$ • One saddle point $(-)$ • One unstable focal fixed point with a limit cycle around it $(+)$
$a_{0,3} \geqslant 0.93$	• One stable fixed point $(-)$ • One saddle point $(-)$ • One unstable focal fixed point with a limit cycle around it $(+)$

one stable fixed point or stable focal fixed point in the $\{v, e\}$ space. The trajectories initiated around the stable fixed point or stable focal fixed point are finally localized at this fixed point. When $-0.16 < a_{0,3} < 0.16$, there are two stable focal points. On the other hand, a limit cycle appears if $a_{0,3} \geqslant 0.16$. In figure 2, we show several phase trajectories on the phase space, $\{v, e\}$, for several values of $a_{0,3}$ which describe different classifications of fixed points as listed in table 1. Here, we note that the overall behavior of this system is not much sensitive to variations of $a_{0,1}$.

To see the pattern of motion for the limit cycle, we replot the phase diagram for $a_{0,3} = 1.2$ in figure 3(a) with corresponding $v(t)$ and $x(t)$ in figures 3(b) and (c), respectively. It shows that the quasi-triangle-shaped limit cycle corresponds to a step-by-step movement of the particle (solid line), while the stable fixed point corresponds to a smooth movement (dashed line). The direction of motion depends on the initial velocity. We will discuss this stepping motion in detail later, because it may be applicable to the molecular motor systems in biology.

Now, we include the fourth order term in the conversion rate, $d(v)$, and analyze the classification of the fixed points as $a_{0,4}$ is varied.

$$d(v) = a_{0,1}v + a_{0,2}v^2 + a_{0,3}v^3 + a_{0,4}v^4. \tag{11}$$

For the numerical analysis, we use $a_{0,1} = 0.0002$, $a_{0,2} = 2.0$, $a_{0,3} = 1.2$, and $f = 0$. We will discuss the effect of the external force later.

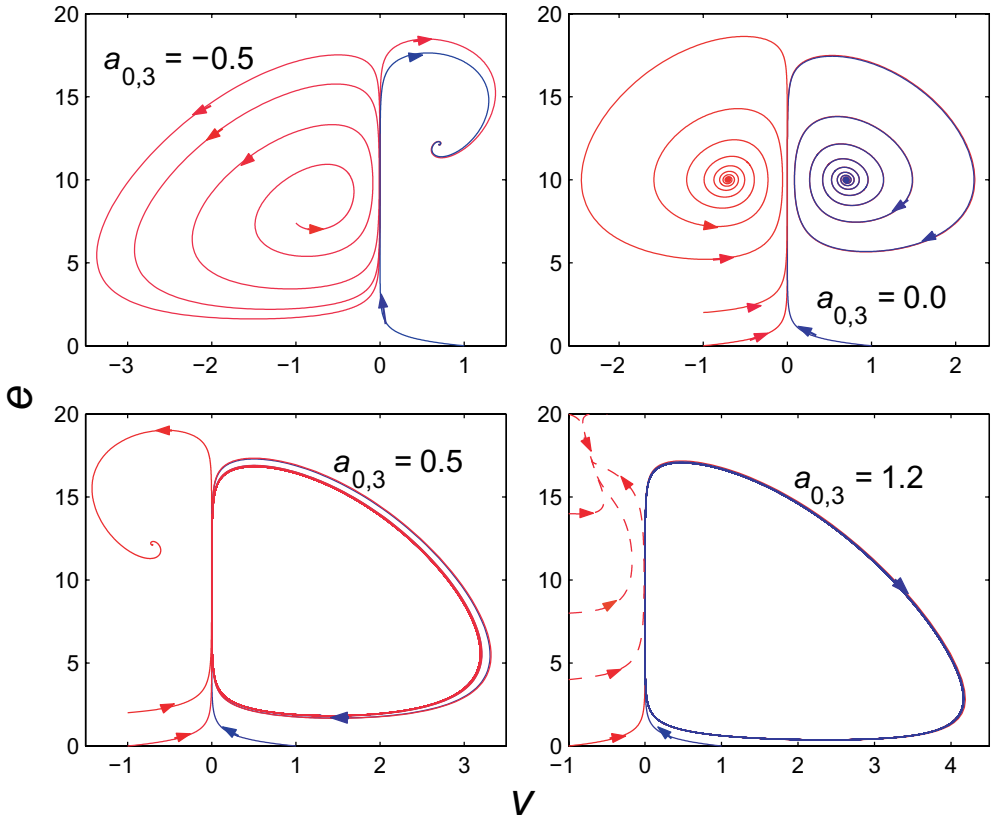

Figure 2. Trajectories in the phase space, $\{v, e\}$, for several values of $a_{0,3}$, when $a_{0,1} = 0.0002$, $a_{0,2} = 2.0$ and $f = 0$. Note that a limit cycle appears only if $a_{0,3} \geqslant 0.16$.

In table 2, the bifurcations and corresponding nature of fixed points for different values of $a_{0,4}$ are listed. When $a_{0,4} < -0.69$, the particle moves smoothly regardless of the initial velocity. As $a_{0,4}$ increases, the motion starts to depend on the initial state of the particle. When $-0.69 \leqslant a_{0,4} < 0.92$, the particle shows a directed stepping motion or a smooth motion depending on the sign of the initial velocity. Interestingly, when $a_{0,4} > 0.92$, the particle moves stepwise in the positive direction eventually regardless of its initial velocity. We plot this behavior in figure 4, when $a_{0,4} = 1.0$.

So far, we have not included any external forces to the system. However, it has been shown that the active particle is able to show a directed motion, without any external forces, depending on the structure of the rate of conversion of the internal energy into the motion. Another interesting feature is that the directed motion could be stepwise. Such a directed stepwise motion appears in the motion of molecular motors in biology. The molecular motors usually carry external loads dictated by their functions. In order to simulate this load-carrying capability of the molecular motors, we now apply an external force, f, to the active particle. To analyze the bifurcation as f varies, we assume that f remains constant during the motion and use that $a_{0,1} = 0.0002$, $a_{0,2} = 2.0$, $a_{0,3} = 1.20$ and $a_{0,4} = 1.0$. Table 3 shows the classification of the fixed points for various ranges of f, where a positive force pulls the particle to the positive direction and a negative force acts as a load against the positive direction of motion.

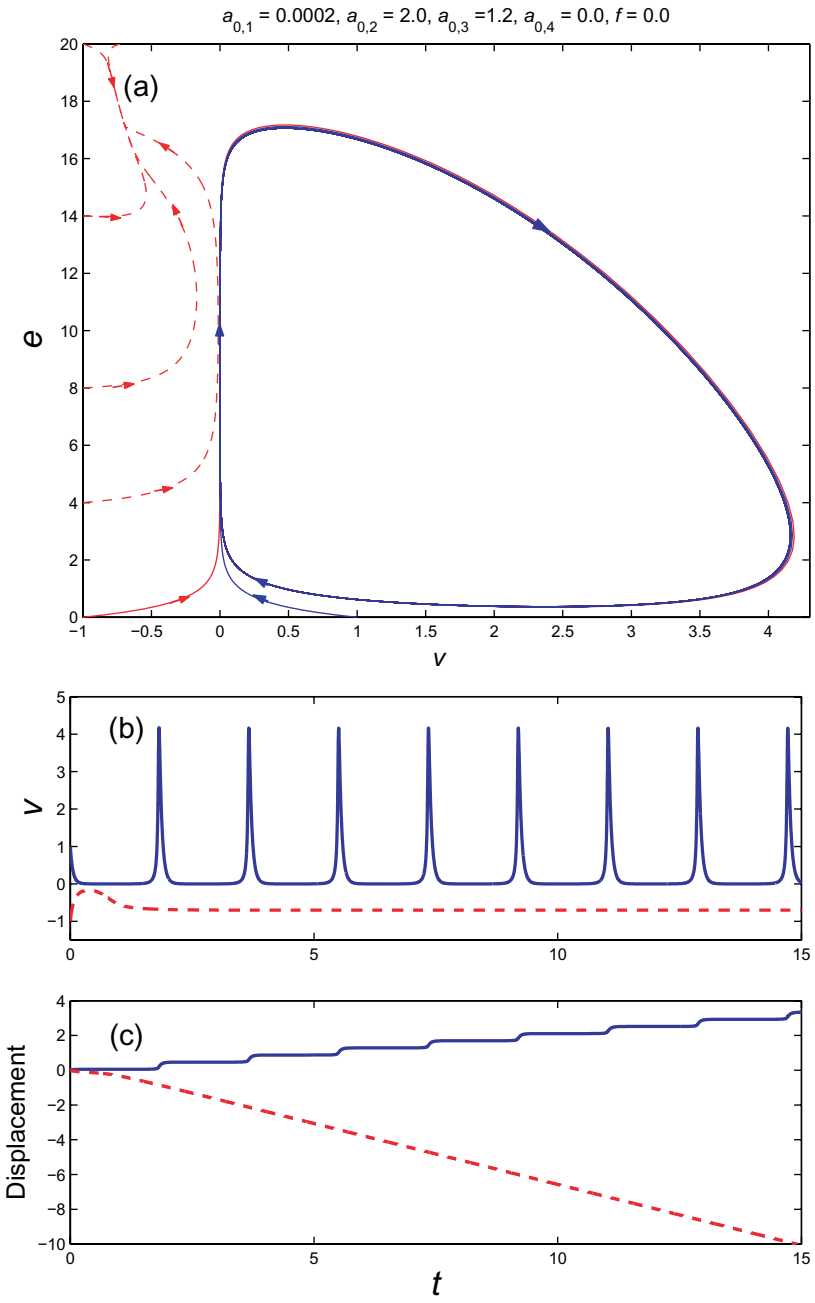

Figure 3. (a) Trajectories in the phase space, $\{v, e\}$, when $a_{0,1} = 0.0002$, $a_{0,2} = 2.00$, $a_{0,3} = 1.2$ and $f = 0$. (b) When the initial velocity is in the positive (negative) direction, the velocity has a steady jerky (smooth) pattern in time. (c) Displacement of the particle is step-like (smooth) for the limit cycle (stable fixed point).

When the load is large enough, $f < -0.89$, a limit cycle does not appear, yielding a smooth movement pulled back. If $-0.89 \leqslant f < -0.85$, the pulled back particle moves stepwise except when it is initialized close to the left fixed point. On the other hand, the particle is pulled back due to the load and moves stepwise regardless of the initial state if $-0.85 \leqslant f < -0.0021$.

Table 2. Bifurcation with a variation of $a_{0,4}$ when $d(v) = a_{0,1}v + a_{0,2}v^2 + a_{0,3}v^3 + a_{0,4}v^4$, $a_{0,1} = 0.0002$, $a_{0,2} = 2.0$, $a_{0,3} = 1.2$ and $f = 0$. Here, (+/−) denotes positive/negative velocity.

Range of $a_{0,4}$	Classification of the fixed point(s)
$a_{0.4} < -1.93$	• One stable fixed point (−) • One saddle point (−) • One stable fixed point (+)
$-1.93 \leqslant a_{0,4} < -0.69$	• One stable fixed point (−) • One saddle point (−) • One stable focal fixed point (+)
$-0.69 \leqslant a_{0,4} < 0.25$	• One stable fixed point (−) • One saddle point (−) • One unstable focal fixed point with a limit cycle around it (+)
$0.25 \leqslant a_{0,4} < 0.92$	• One stable focal fixed point (−) • One saddle point (−) • One unstable focal fixed point with a limit cycle around it (+)
$0.92 \leqslant a_{0,4} < 2.89$	• One unstable focal fixed point (−) • One saddle point (−) • One unstable focal fixed point with a limit cycle around it (+)
$a_{0,4} \geqslant 2.89$	• One unstable fixed point (−) • One saddle point (−) • One unstable focal fixed point with a limit cycle around it (+)

Note that the saddle point moves from $v > 0$ (when $f < -0.2$) to $v < 0$ (when $-0.2 < f$) by crossing the value $v = 0$ when $f = -0.2$. In a very narrow range, $-0.0021 \leqslant f < -0.0019$, the particle is able to move stepwise in both negative and positive directions depending on the initial state. When $-0.0019 < f \leqslant 5.38$, the particle can overcome the load and move stepwise to the opposite direction of the load. For a sufficiently large force in the positive direction, the particle is dragged smoothly to the same direction of the force regardless of the initial state of the particle. We plot these trajectories in figure 5.

5. Stepping motion

The limit cycle in our phase space, $\{v, e\}$, indicates a stepwise motion in time. Moreover, a particle carrying a load (f, in this model) can perform a directed step-by-step motion overcoming the load. This motion is similar to that of a processive molecular motor in a cell.

Table 3. The bifurcation with the variation of the external force when $a_{0,1} = 0.0002$, $a_{0,2} = 2.0$, $a_{0,3} = 1.2$ and $a_{0,4} = 1.0$. Here, $(+/-)$ denotes positive/negative velocity.

Range of f	Classification of the fixed point(s)
$f \leqslant -2.77$	• One stable focal fixed point $(-)$ • One saddle point $(+)$ • One unstable fixed point $(+)$
$-2.77 < f < -0.89$	• One stable focal fixed point $(-)$ • One saddle point $(+)$ • One unstable focal fixed point $(+)$
$-0.89 \leqslant f < -0.85$	• One stable focal fixed point with a limit cycle around it $(-)$ • One saddle point $(+)$ • One unstable focal fixed point $(+)$
$-0.85 \leqslant f < -0.2$	• One unstable focal fixed point with a limit cycle around it $(-)$ • One saddle point $(+)$ • One unstable focal fixed point $(+)$
$f = -0.2$	• One unstable focal fixed point with a limit cycle around it $(-)$ • One saddle point at the resting state $(v = 0)$ • One unstable focal fixed point $(+)$
$-0.2 < f < -0.0021$	• One unstable focal fixed point with a limit cycle around it $(-)$ • One saddle point $(-)$ • One unstable focal fixed point $(+)$
$-0.0021 \leqslant f \leqslant -0.0019$	• One unstable focal fixed point with limit a cycle around it $(-)$ • One saddle point $(-)$ • One unstable focal fixed point with a limit cycle around it $(+)$
$-0.0019 < f \leqslant 5.38$	• One unstable focal fixed point • One saddle point $(-)$ • One unstable focal fixed point with a limit cycle around it $(+)$
$5.38 < f < 6.496$	• One unstable focal fixed point $(-)$ • One saddle point $(-)$ • One stable focal fixed point $(+)$
$f \geqslant 6.496$	• One unstable fixed point $(-)$ • One saddle point $(-)$ • One stable focal fixed point $(+)$

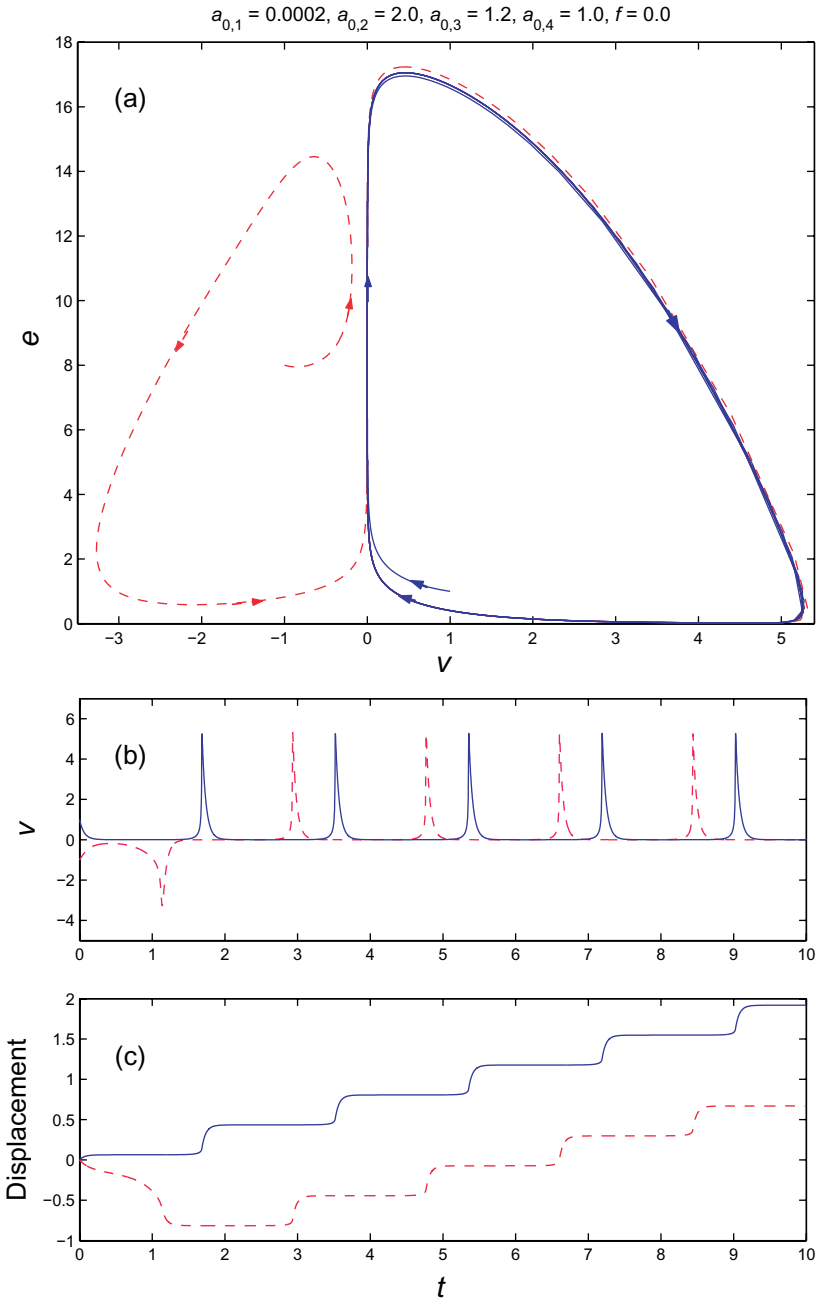

Figure 4. Trajectories when $a_{0,1} = 0.0002$, $a_{0,2} = 2.0$, $a_{0,3} = 1.2$, $a_{0,4} = 1.0$ and $f = 0$. (a) The phase diagram of the particle in the $\{v, e\}$ space. As shown in table 2, there is one limit cycle around the fixed point with the positive velocity. (b) The velocity is jerky regardless of the direction of the initial velocity. (c) The particle shows stepping motions to the positive direction even for the initial motion of negative velocity.

Here, we analyze an engine mechanism of the limit cycle and relate it to the walking mechanism of the molecular motors. The effect of noise on the stepping motion in our generalized energy-depot model is also discussed.

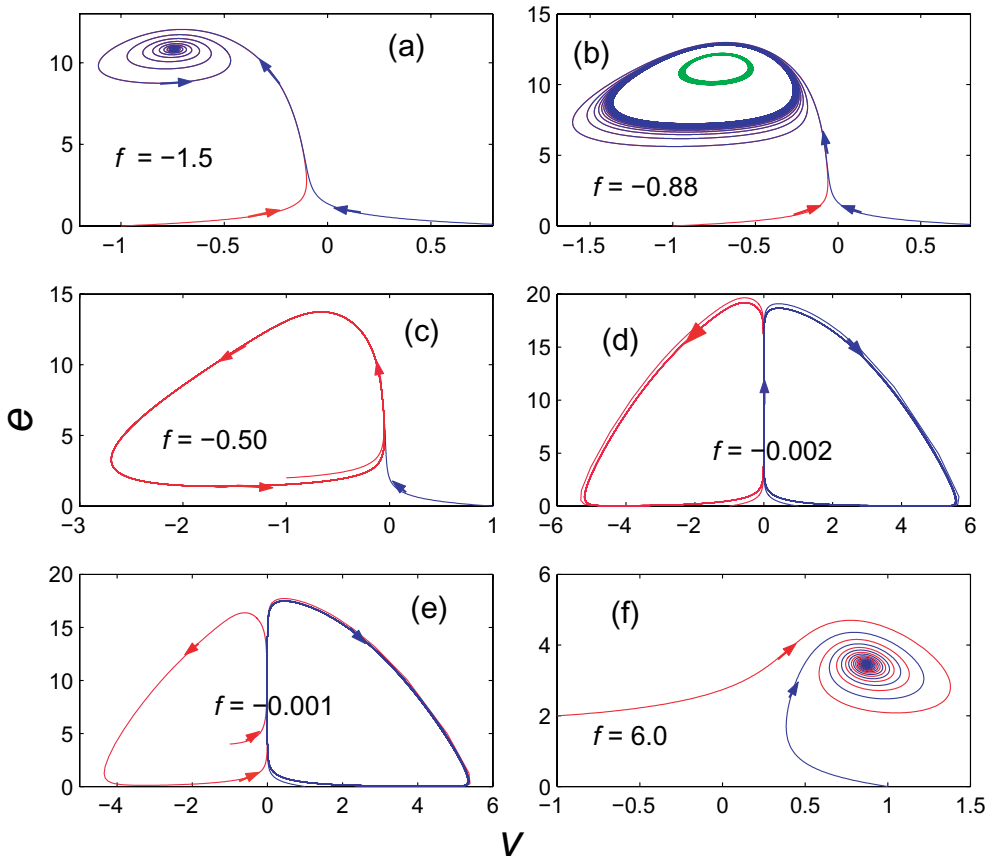

Figure 5. Trajectories in the phase space, $\{v, e\}$ for several values of f chosen from table 3, when $a_{0,1} = 0.0002$, $a_{0,2} = 2.0$, $a_{0,3} = 1.2$ and $a_{0,4} = 1.0$. (a) The particle is pulled back in a smooth way due to a heavy load. (b) The pulled back particle moves stepwise except when it is initialized close to the left fixed point. (c) The particle is pulled back due to the load and moves stepwise regardless of the initial state. (d) The particle is able to move stepwise in both negative and positive directions depending on the initial state. (e) The particle can overcome the load and move stepwise to the positive direction. (f) A sufficiently large force to the positive direction drags the particle smoothly to the positive direction regardless of the initial state of the particle.

Figure 6 shows the typical pattern of the limit cycle appearing in our model. This triangle-like limit cycle describes cycling motions between three states: resting ($\dot{e} > 0$, $\dot{v} = 0$), accelerating ($\dot{e} < 0$, $\dot{v} > 0$) and decelerating ($\dot{e} \sim 0$, $\dot{v} < 0$) states. The energy is supplied during the resting state, consumed during the acceleration, and barely changed during the deceleration. Hence, cyclic repetition of this motion leads to the stepping motion as mentioned in the previous sections.

To explain the walking mechanisms of molecular motors such as kinesin and myosin V, a three-state model has been proposed [24, 25]. The three-state model describes 'ATP binding' to the motor at rest, 'ATP hydrolysis and movement' and 'attachment and ADP-releasing'. The 'ATP binding' plays the role of the energy input ($\dot{e} > 0$) while stalling ($\dot{v} = 0$), and the 'ATP

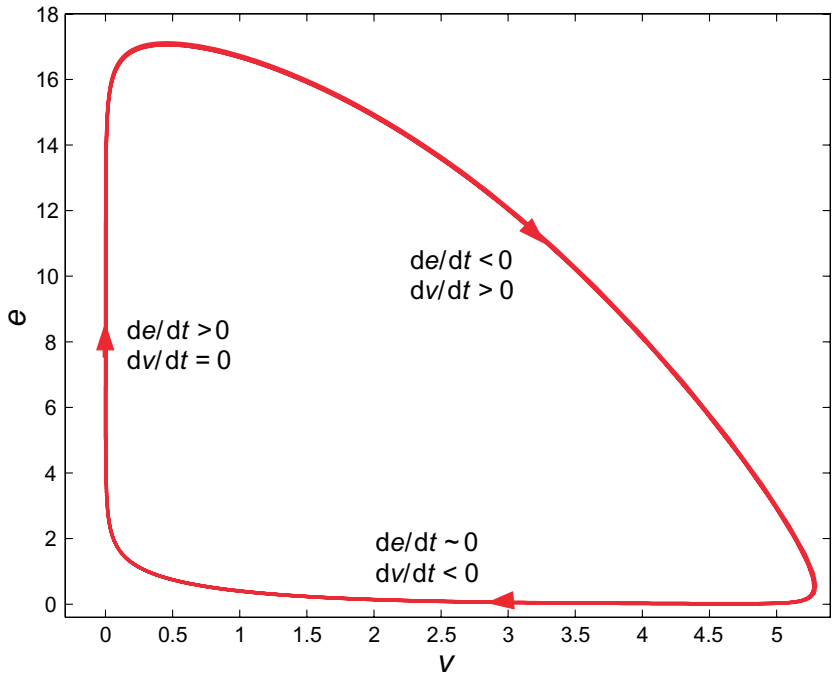

Figure 6. The engine mechanism of the limit cycle. The motion can be approximately divided into three states: resting ($\dot{e} > 0$, $\dot{v} = 0$), accelerating ($\dot{e} < 0$, $\dot{v} > 0$) and decelerating ($\dot{e} \sim 0$, $\dot{v} < 0$) states.

hydrolysis and movement' corresponds to the energy consumption ($\dot{e} < 0$) for the acceleration ($\dot{v} > 0$) in our model. When ADP is released, there is no energy cost. Hence, the 'attachment and ADP-releasing' state corresponds to the decelerating state ($\dot{e} = 0$, $\dot{v} < 0$) in our model. The difference between the three-state model for the molecular motor and our generalized energy-depot model is that the molecular motors are walking on tracks such as microtubules or actin filaments. However, the interaction between the motor protein and the microtubule or the actin filament can be considered in our model by introducing the corresponding external force. We will report on this in a later work.

So far, we have neglected the contribution of stochastic noise to the motion of the active particles. However, the thermal fluctuation is inevitable and expected to play an important role especially in the motion of the molecular motors and nano-robots. Hence we include the stochastic term with the noise strength $\sqrt{2k_{\mathrm{B}}T\mu_0}$ in the calculation of the motion. We calculate the effect of the stochastic noise on the stepping motions described in figures 5(d) and (e) in which the applied loads are $f = -0.002$ and $f = -0.001$, respectively. The stochastic stepping motions are plotted in figure 7, when the strength of the noise is 0.6. As expected, the particle can move forward or backward as a consequence of the noise fluctuation, yielding irregularly directed stepwise motion as observed in the motion of the molecular motors [15]–[17]. Here, we compare the present work with the existing studies on the directed motion of active particles [10]–[12]. In those works, the asymmetry of space was described by an external rachet potential [10]–[12]. However, in our model, this asymmetry is given by the conversion function, i.e. the energy depot itself. In our model, the noise introduces occasional backward motion as observed in experiments [15]–[17], unlike previous models. Therefore, further study of the

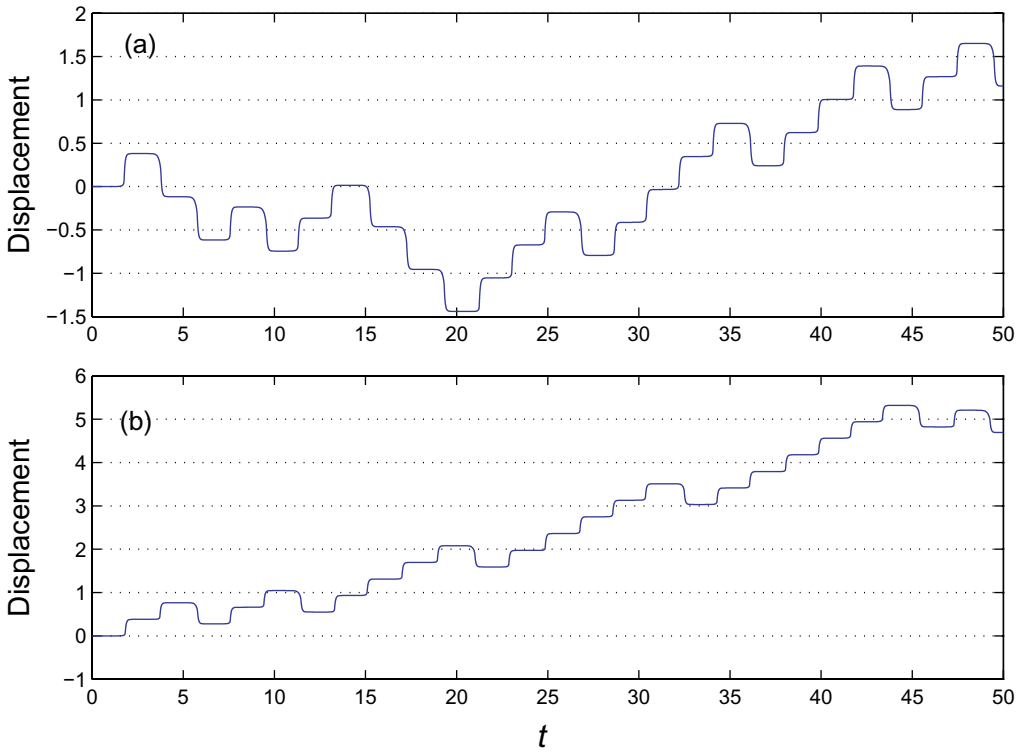

Figure 7. The stochastic stepping motion of the active particle with a constant load f when $a_{0,1} = 0.0002$, $a_{0,2} = 2.0$, $a_{0,3} = 1.2$, $a_{0,4} = 0.93$, and the noise strength is 0.6; (a) $f = -0.002$ and (b) $f = -0.001$.

effect of the external ratchet potential on the present model appears necessary to understand the physical origin of the motional polarity.

6. Negative stiffness

The rate of conversion of the internal energy into the motion is in general a function of space and velocity [9, 20]. As we have observed that the velocity-dependent conversion rate can induce an active behavior in a certain velocity range, it is expected that a position-dependent conversion rate may also introduce an active behavior in oscillation. In this section, we consider a special form of the space-dependent conversion rate to show that our generalized energy-depot model induces an active behavior in a certain spatial range. This active behavior in an oscillatory system appears as the negative stiffness of the membrane or bundle. As an example, it is known that the spontaneous oscillation of the mechanosensitive hair bundle in the inner ear is strongly related to the negative stiffness of the bundle [18]. Therefore, we believe that it is desirable to investigate contributions from a conversion rate function, which depends on velocity and position simultaneously.

Motivated by this observation, we consider the following form of the conversion rate,

$$d(x, v) = a_{1,1} x v + a_{3,1} x^3 v. \tag{12}$$

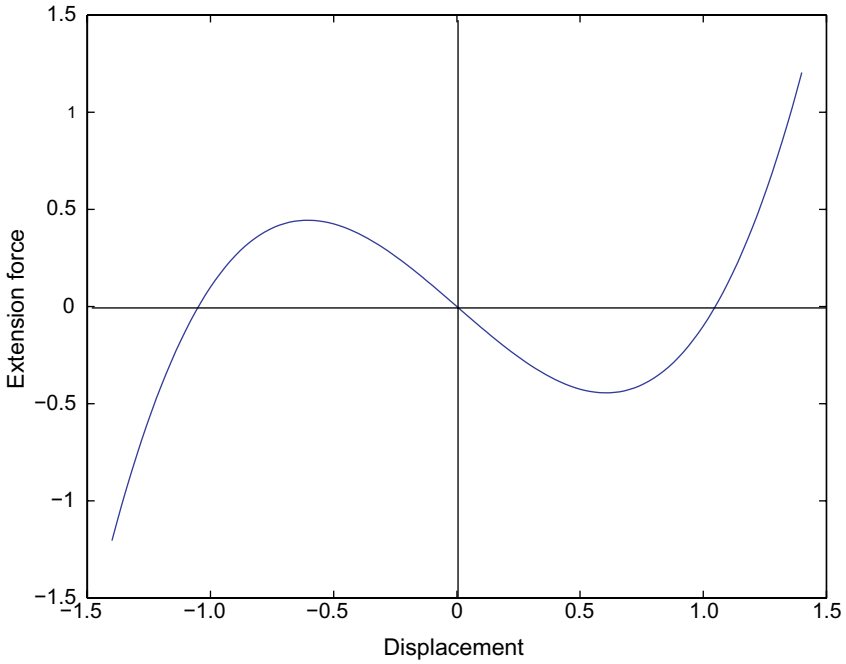

Figure 8. Extension force $\kappa_{\text{eff}}x$ versus x when $d(x, v) = a_{1,1}xv + a_{3,1}x^3v$. In this plot, we use that $a_{1,1} = 2.1$, $a_{3,1} = -1$, $\kappa = 1$, and $e = 1$.

For the stationary state, $\dot{e} = 0$, the equation of motion becomes

$$m\dot{v} = -\mu_0 v - \kappa_{\text{eff}}x + f, \tag{13}$$

where the effective stiffness is

$$\kappa_{\text{eff}} = \kappa - (a_{1,1} + a_{3,1}x^2)e. \tag{14}$$

To avoid infinite amplitude of vibration, $a_{3,1}$ should be negative. Note that if the second term exceeds the physical stiffness κ, κ_{eff} could be negative in the region $-\sqrt{(a_{1,1}e - \kappa)/|a_{3,1}|e} < x < \sqrt{(a_{1,1}e - \kappa)/|a_{3,1}|e}$. Figure 8 plots the extension force $\kappa_{\text{eff}}x$ versus x. This type of negative stiffness has been experimentally observed and explained using a two-state model [18]. Thus, it will be interesting to investigate possible connections between the position-dependent conversion rate and the two-energy-state model. Another possible application of the position-dependent conversion rate is introduction of a protective mechanism for the system from excessive displacement. We believe that a suitable choice of the conversion rate can provide such a protective mechanism for oscillatory nano-robots.

7. Conclusion

In this paper, we have presented a general model of an active Brownian particle in which the rate of conversion of the internal energy into motion is a general function of the velocity of the particle. We have shown that when the conversion rate depends only on v^2 and v^4, an active amplification and a protective braking mechanism appear. We believe that this active

amplification with a braking mechanism can provide a new paradigm for any underdamped biological system and nano-machine. It is conceivable that the evolutionary tactic in biological systems may have provided such protective mechanisms to any underdamped biological units to protect them from excessive oscillations. Such a self-adapting mechanism will also be needed in designing nano-machines.

When the conversion rate is asymmetric in velocity, various interesting behaviors appear. One of the most remarkable behaviors is a directed motion without any external forces. Such a directed motion suggests the possibility of overcoming any extra load on the particle. Another very remarkable behavior is a stepping motion described as a limit cycle. Such a stepping motion has a polarity and, hence, is applicable to molecular motors.

When the conversion rate depends not only on the velocity but also on the position of the particle, it has been shown, for a very special case, that the effective stiffness of an oscillatory system could be negative. Such a behavior has been observed in hair bundle motion in the inner ear. Hence it also suggests the possible connection between our generalized energy-depot model and a relevant biological system.

We have shown that various interesting active motions that exist in the real world can be induced for active Brownian particles by considering various forms of the conversion of energy into motion. It is quite remarkable that our general energy-depot model could describe such a variety of motions even though the generic relations between our model and the real world have to be investigated further.

Acknowledgments

We thank Professors Yongah Park and Myung-Hoon Chung for fruitful discussions. This work was supported by a Korea Science and Engineering Foundation (KOSEF) grant funded by the Ministry of Education, Science and Engineering (MEST), Korea (R01-2006-000-10083-0).

References

[1] Mahadevan L and Matsudaira P 2000 *Science* **288** 95
[2] Skotheim J M and Mahadevan L 2005 *Science* **308** 1308
[3] Mach R and Schweitzer F 2007 *Bull. Math. Biol.* **69** 539
[4] Shibona G J 2007 *Phys. Rev.* E **76** 011919
[5] Chang S T, Paunov V N, Petsev D N and Velev O D 2007 *Nat. Mater.* **6** 235
[6] Parrish J K, Viscido S V and Grunbaum D 2002 *Biol. Bull.* **202** 296
[7] Toner J, Tu Y and Ramaswamy S 2005 *Ann. Phys.* **318** 170
[8] Schweitzer F, Ebeling W and Tilch B 1998 *Phys. Rev. Lett.* **80** 5044
[9] Schweitzer F 2003 *Brownian Agents and Active Particles* (Berlin: Springer) and references therein
[10] Tilch B, Schweitzer F and Ebeling W 1999 *Physica* A **273** 294
[11] Schweitzer F, Tilch B and Ebeling W 2000 *Eur. Phys. J.* B **14** 157
[12] Ebeling W, Gudowska-Nowak E and Fiasconaro A 2008 *Acta Phys. Pol.* B **39** 1251
[13] Halloy J *et al* 2007 *Science* **318** 1155
[14] Zhang Y, Kim C K, Lee K J B and Park Y 2008 *Eur. Phys. J.* E submitted
[15] Svoboda K, Schmidt C F, Schnapp B J and Block S M 1993 *Nature* **365** 721
[16] Reck-Peterson S L, Yildiz A, Carter A P, Gennerich A and Zhang N 2006 *Cell* **126** 335
[17] Park H, Toprak E and Selvin P R 2007 *Q. Rev. Biophys.* **40** 87

[18] Goff L L, Bozovic D and Hudspeth A J 2005 *Proc. Natl Acad. Sci. USA* **102** 16996
[19] Lindner B 2007 *New J. Phys.* **9** 136
[20] Glücle A and Hüffel H 2008 *Phys. Lett.* B **659** 447
[21] Cikarek S R and Baikey K E 2002 *Proc. Am. Control Conf.* **4** 3129
[22] Rayleigh J W S 1976 *The Theory of Sound* (London: Macmillan)
[23] Strogatz S H 1994 *Nonlinear Dynamics and Chaos* (Reading, MA: Addison-Wesley)
[24] Rief M, Rock R S, Mehta A D, Mooseker M S, Cheney R E and Spudich J A 2000 *Proc. Natl Acad. Sci. USA* **97** 9482
[25] Walker M L, Burgess S A, Sellers J R, Wang F, Hammer J A, Trinick J and Knight P J 2000 *Nature* **405** 804